NANO LETTERS

2008
Vol. 8, No. 10
3394-3397

Microwave Induced In-Situ Active Ion Etching of Growing InP Nanocrystals

Derek D. Lovingood and Geoffrey F. Strouse*

Department of Chemistry and Biochemistry, Florida State University, Tallahassee, Florida 32306-4390

Received July 14, 2008; Revised Manuscript Received July 25, 2008

ABSTRACT

High quantum yield (47%) InP nanocrystals can be prepared without the need for post HF treatment by combining microwave methodologies with the presence of a fluorinated ionic liquid. Growing the InP nanocrystals in the presence of the ionic liquid 1-hexyl-3-methyl-imidazolium tetrafluoroborate (hmim BF_4) allows in situ etching to be achieved. The optimization of the PL QY is achieved by balancing growth and etching rates in the reaction.

The size dependent optical properties of colloidal semiconductor nanocrystals are ideal for applications in fields ranging from biological imaging[1−4] to photovoltaics.[5−7] Due to the ease of synthesis, a significant fraction of the research to date has centered on the II−VI family of semiconductors utilizing the type I core−shell structures, namely, CdSe/ZnS.[8,9] Recent interest has focused on developing routes to the III−V family, namely InP,[10−13] because of the perceived lower toxicity for InP based nanocrystals.[3,10,14−17] The downside to InP is the poor photoluminescence (PL) quantum yield (QY), which is typically <4% once isolated from the reaction mixture, although core−shelling yields a value of ∼20% depending on size.[13,18] The poor PL QY for these materials can be traced to the presence of phosphorus vacancies[12] (V_P) in the material. Removal of the surface V_P sites by active ion etching with hydrofluoric acid (HF) improves the PL performance of these materials to ∼40%.[11,12,19,20] Active ion etching of InP nanocrystals with HF is believed to improve the QY via removal of P dangling bonds that arise from the P rich faces of the growing nanocrystal. By etching away the P faces in the form of PF_3, an In rich face is exposed that provides for more efficient passivation.[11,12] The process is believed to be enhanced by photoactivation via an electron transfer step, although HF etching without light also produces PL enhancement.[19] The use of active ion etching with HF enhances the InP nanocrystal PL, it represents an inconvenient extra synthetic step that lowers solubility, broadens the excitonic absorption line width, and increases the difficulty for ZnS shelling. The development of an in situ active ion etchant can simplify the preparation of this family of material, improve the PL QY, and maintain the optical properties of the nanocrystal.

In this manuscript, a microwave induced in situ active ion etching process is demonstrated that improves the out-of-batch optical performance of InP nanocrystals, although the methodology is likely to be applicable to a wider range of nanocrystals. In situ active ion etching is achieved by adapting our previously developed microwave (MW) based synthetic protocol[11] by the addition of the ionic liquid (IL) 1-hexyl-3-methyl-imidazolium tetrafluoroborate (hmim BF_4). In situ generation of F^- (active ion) is achieved through direct MW absorption by the IL, thermal relaxation to the fluoride containing counterion, and subsequent production of F^- resulting in V_p removal during the growth of the InP nanocrystal. The photoluminescence quantum yield (PL QY) for InP grown under in situ etching conditions is 47% for the additive hmim BF_4 at a mole ratio of 1:10 (In^{3+} to IL). Time dependent degradation studies of the InP grown with the IL indicates the PL properties are maintained in solution for an extended time frame with no detectable change in PL QY after 24 h. The in situ microwave assisted active ion etching method represents the first technique to produce high PL QY InP nanocrystals out of batch without using post HF treatment or core−shelling. More importantly, it points to a methodology that allows in situ vacancy or defect removal during the chemical preparation of nanocrystals.

The use of ionic liquids in synthesis have attracted attention due to the high thermal stability of the solvent, nonreactivity of the materials, and the added benefit of the solvent being recyclable.[21] In an earlier report, our group demonstrated the advantages of using nonfluorinated ionic liquids in MW chemistry to accelerate growth of InP and CdSe nanocrystals.[11] The isolated InP showed typical PL QYs for this family with values on the order of 4%. Following HF treatment, the PL QY increases to 38%.[11] The most notable effect of using an ionic liquid in MW chemistry

* Corresponding author. Phone: 850-645-1898. Fax: 850-645-8281. E-mail: strouse@chem.fsu.edu.

10.1021/nl802075j CCC: $40.75
Published on Web 09/13/2008

Table 1. Additives Used in InP Synthesis

anion	additive	abbreviation	ratio	PL QY	ramp time (sec)
$[BF_4]^-$	1-hexyl-3-methyl-imidazolium BF_4	hmim BF_4	1:20	35.3	55
		hmim BF_4	1:10	47.1	70
		hmim BF_4	1:5	41.6	225
		hmim BF_4	1:3	34.6	410
		hmim BF_4	1:2	8.8	340
		hmim BF_4	1:1	1.7	760
		hmim BF_4	1:0.1	1.2	810
	1-butyl-4-methyl-pyridinium BF_4	bmpy BF_4	1:20	29.5	180
		bmpy BF_4	1:10	43.2	220
		bmpy BF_4	1:5	9.9	250
		bmpy BF_4	1:3	2.7	325
		bmpy BF_4	1:2	3.8	435
		bmpy BF_4	1:1	1.6	590
		bmpy BF_4	1:0.1	1.3	1320
	tetrabutylammonium BF_4	TBA BF_4	1:10	11.2	170
		TBA BF_4	1:1	4.2	370
		TBA BF_4	1:0.1	1	1735
[PF6]$^-$	1-hexyl-3-methyl-imidazolium PF_6	hmim PF_6	1:10	24.5	150
		hmim PF_6	1:1	5.7	310
		hmim PF_6	1:0.1	1.8	485
	1-butyl-4-methyl-pyridinium PF_6	bmpy PF_6	1:10	N/A	220
		bmpy PF_6	1:1	1.8	302
		bmpy PF_6	1:0.1	1	485
	tetrabutylammonium PF_6	TBA PF_6	1:10	N/A	305
		TBA PF_6	1:1	1	432
		TBA PF_6	1:0.1	1	1065
F^-	tetrabutylammonium fluoride	TBA F	1:10	N/A	190
		TBA F	1:1	N/A	295
		TBA F	1:0.1	1	720
Cl^-	1-hexyl-3-methyl-imidazolium Cl	hmim Cl	1:10	N/A	135
		hmim Cl	1:1	N/A	430
		hmim Cl	1:0.1	2.3	670
	1-butyl-4-methyl-pyridinium Cl	bmpy Cl	1:10	N/A	140
		bmpy Cl	1:1	N/A	494
		bmpy Cl	1:0.1	1.5	1332

is the efficient conversion of MW energy into thermal energy due to the high MW cross section that ionic liquids possess. In MW chemistry, the molecule with the highest cross section selectively absorbs the MW energy and, through relaxation, heats the solvent or the molecular precursors. The selective absorption leads to the "specific" microwave effects often quoted in the synthetic literature.[22] Ionic liquids typically are not directly involved in the reaction mechanism and can be considered a spectator solvent, allowing nonabsorbing materials to be rapidly heated in the MW by convective loss, although ILs are believed to enhance reactions due to the highly ordered solvent framework.[21,23] Choosing an ionic liquid containing a fluorinated anion that thermally degrades would circumvent the HF step by directly producing an in situ F^- source. The concentration of F^- would be controlled by the MW absorption cross section of the IL and subsequent thermal degradation of the fluoride source.

It is well-known from the literature that $[PF_6]^-$ and $[BF_4]^-$ anions are prone to thermal decomposition producing controlled quantities of F^- ions. The thermal production of fluoride ions arises from a Balz-Schiemann type reaction.[24−26] In fact, it has been shown that tetrafluoroborate based ionic liquids thermally decompose at 240 °C at a rate of 0.017%/min.[27] In order to assess the affect on the PL QY of InP by the addition of fluorinated ILs during nanocrystal growth, we have investigated a series of ILs based on 1-hexyl-3-methyl-imidazolium (hmim), 1-butyl-4-methyl-pyridinium (bmpy), and tetrabutylammonium (TBA) with the counterions $[BF_4]^-$, $[PF_6]^-$, F^-, and Cl^- (Table 1).

The InP nanocrystals are prepared by injecting separate stock solutions of indium palmitate and tris-trimethylsilylphosphine $[(TMS)_3P]$ dissolved in decane into a microwave reactor vessel containing fixed concentrations of the additive in Table 1. The synthetic method is an extrapolation of literature procedures[10,11] using separate stock solutions of the precursors that are mixed prior to MW irradiation. MW growth is accomplished by ramping the reaction at 300 W (single mode, focused, 2.45 GHz) using a CEM Discover microwave reactor. The general parameters used in this work are as follows: (1) reaction power of 300 W (ramping time from 1−25 min depending on additives), (2) reaction temperature at 280 °C, and (3) reaction time of 15 min with "active cooling" of the microwave cavity to remove latent heat. It should be noted that the ramping conditions may vary depending on the choice of additives or MW system used. Once the MW reaction is complete, the temperature is rapidly reduced to room temperature (∼2 min)

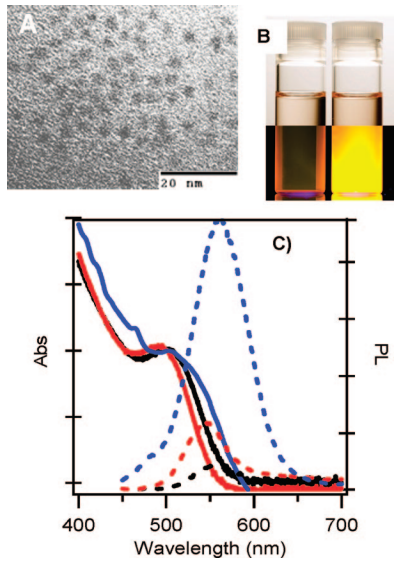

Figure 1. (A) TEM of grown InP with hmim BF_4. (B) Optical image comparing the solution of InP nanocrystals (hexane) for materials grown with and without hmim BF_4 (1:10 mol ratio). The lower half of the image is under UV irradiation. (C) Comparison of Abs and PL of InP grown with hmim BF_4. Concentrations of the In^{3+} precursor to the IL used are 1:0.1 (black), 1:1 (red), and 1:10 (blue).

using forced air cooling. For the optical studies, the InP nanocrystals are isolated from the reaction mixture by initial addition of toluene and precipitation by addition of acetone, followed by treatment with toluene/MeOH (two times). The quantum yields were determined by comparing the emission of InP with that from rhodamine 6G in ethanol (QY = 95%), as described previously.[11]

Using TEM, the MW grown InP are 2.7 ± 0.3 nm spherical, Zn- blende (cubic) morphology nanocrystals (Figure 1A). The large disparity represents an upper limit due to imaging imitations for these materials at this size regime. pXRD analysis (Supporting Information Figure 1) of the sample indicates a Zn-blende structure ($F\bar{4}3m$) is formed. Scherrer analysis of the pXRD confirms the TEM size measurement. ^{19}MAS solid state nuclear magnetic resonance spectroscopy (Supporting Information Figure 2) shows that fluorine is still present after material isolation on the InP samples grown by these methods. This is in agreement with InP that has been HF etched.[12]

The magnitude of enhancement resulting from adding hmim BF_4 to the MW reactor is clearly evidenced in the dramatic PL improvement observed for the InP nanocrystal grown in the presence and absence of the IL (Figure 1B). The changes in the absorption and PL spectra for InP grown with the additive added in a 1:0.1, 1:1, and 1:10 mol ratio of In^{3+} to hmim BF_4 are shown in Figure 1C. The PL QYs for each additive condition is compiled in Table 1. The $[BF_4]^-$ salts showed the highest overall PL QY improvement, the $[PF_6]^-$ based ILs produced lower QYs, while the F^- and Cl^- salts did not produce highly emissive materials or led to loss of the nanocrystal.[28] The highest PL QY arises for the ionic liquid hmim BF_4 at a concentration of 1:10. At this concentration, it was possible to reproducibly grow InP

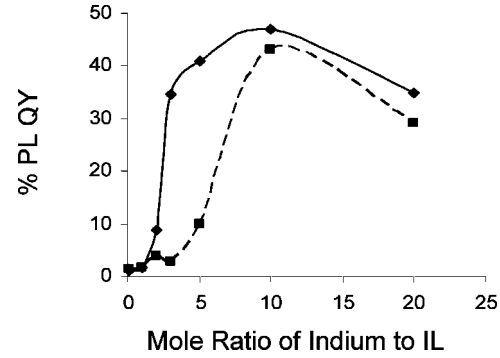

Figure 2. PL QY for a series of In^{3+}:IL mole ratios of InP grown with hmim BF_4 (solid) and InP grown with bmpy BF_4 (dash).

with a PL QY of 47%. No spectral shift for the PL profile is observed for the various concentrations of hmim BF_4 (Figure 1C) or bmpy BF_4 (Supporting Information Figure 3); however, as the concentration of IL is increased, the InP PL QY asymptotes for the hmim BF_4 at a concentration above 1:5, while bmpy BF_4 asymptotes at 1:10 (Figure 2). The difference in hmim and bmpy can be explained due to the higher polarity of hmim and therefore higher MW absorption and subsequent thermal transfer from the IL to the counterion.[29] The higher thermal transfer leads to higher fluoride ion release in the reaction.

The observed InP PL QY depends on both the IL and the concentration of IL. For samples grown with a 1:10 mol ratio of the IL, the trend observed is $BF_4^- > PF_6^- \gg Cl^-$, while at a 1:1 ratio, the PL QY follows the trend $PF_6^- > BF_4^- \gg Cl^-$ (Figure 3). The observed anion dependence on IL mole ratio reflects the magnitude of F^- production, with $[PF_6]^-$ having the highest fluoride ion production in time compared with $[BF_4]^-$. The level of fluoride ion production mirrors the bond energies for the B−F bond (174 kcal/mol) compared with the P−F bond (96 kcal/mol).[30] The weaker bond strength in P−F will result in more facile thermal degradation and therefore higher fluoride ion concentrations. At high IL mole ratios, the increased fluoride ion concentration leads to aggressive etching and subsequent loss of the materials.

To assess whether the PL improvement requires an IL with a high MW cross section or just an anion capable of producing fluoride ion, TBA salts of $[BF_4]^-$, $[PF_6]^-$, and F^-

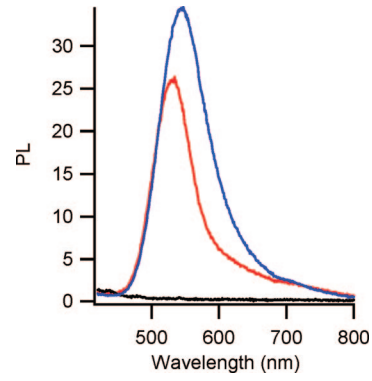

Figure 3. Comparison of PL properties for InP grown with a 1:1 mol ratio of hmim PF_6 (blue), hmim BF_4 (red), and hmim Cl (black).

were tested at a reaction temperature of 280 °C, which is high enough to initiate anion degradation. Inspection of Table 1 illustrates that the combination of IL and counterion is necessary to achieve high PL QY in these materials. Although PL QY improvement is observed for TBA BF_4, the PL QY for TBA BF_4 was far lower (11%) than that observed for either hmim BF_4 (47%) or bmpy BF_4 (43%). For the TBA salts, the magnitude of PL QY followed the trend $[BF_4]^- \gg [PF_6]^- \sim F^-$. At high concentrations of the $[PF_6]^-$ or F^- salts, the InP nanocrystals are not formed. As noted earlier, it is believed that, for the $[PF_6]^-$ and F^- salts, more rapid fluoride generation exists in the reaction and the resultant F^- ions inhibit InP growth due to formation of InF_3 and reaction with the P source with subsequent formation of PF_3. The difference in PL QY between TBA and hmim can be explained because of the lower microwave absorption by TBA during the reaction resulting in lower F^- production for the ILs during the InP growth. The lower MW cross section for TBA is clearly evidenced by the longer MW ramp times observed for the TBA salts (Table 1).

The experimental results suggest that a slow, controlled production of fluoride ions during nanocrystal growth is crucial to produce the highest PL QY in InP. The slow production of fluoride ions apparently allows controlled removal of defects to compete with nanocrystal growth. The actual mechanism of etching is presumed to follow a similar pathway as observed in Si nanocrystals[31] and InP nanocrystals,[12,19] where the presence of HF leads to removal of oxidized P or enhances the cleavage of the Si−P bond, which arises from the P^{3-} precursor (TMS_3P). The oxidized P sites likely are generated by thermal decomposition of In−palmitate or the In−acetate precursor. Alternatively, excess F^- ions may also interact with dangling P ions at the nanocrystal surface, consistent with the NMR results and our previous observations[11] (Supporting Information Figure 2). At high fluoride ion concentrations ($[PF_6]^-$ vs $[BF_4]^-$), the rate of etching is faster than the rate of the growth resulting in poor material performance. At low fluoride ion content (hmim BF_4 vs bmpy BF_4), the reaction results in faster growth than etching, which yields poor PL QYs. The balance of etching and growth imply that during synthesis of InP nanocrystals an ionic liquid with a fluoride counterion serves two functions: (1) to superheat the reaction due to the high absorption cross section for microwave energy of the IL converting that energy to convective energy, and (2) production of a transient in situ source for fluoride ions by thermal degradation of the counterion. MW chemistry allows the careful control of etching relative to growth by balancing the MW cross section of the reactants with the thermal degradation rate for the fluoride containing IL. The careful control provided by the MW leads to a rapid, convenient, synthetic methodology allowing isolation of InP nanocrystals with nearly 50% PL QYs that is adaptable to a flow through technology.[32] Such a technology may open the use of these materials in bioimaging applications where toxicity issues are a concern for bionanotechnology.

Acknowledgment. Funding was provided by the National Institute of Health through NIH EB-R01-00832 and the National Science Foundation through NSF-DMR-0701462. We thank Dr. Randall Achey of the Florida State University NMR facility for his assistance and discussion related to solid state NMR. We also thank Dr. Yan Xin of the National High Field Magnetic Laboratory (NSF-DMR 9625692) for assistance with TEM.

Supporting Information Available: pXRD spectra of InP grown with hmim BF_4 and bmpy BF_4 (Supplemental Figure 1), PL of InP grown with bmpy BF_4 (Supplemental Figure 2), and ^{19}F MAS spectra of InP grown with bmpy BF_4 (Supplemental Figure 3). This material is available free of charge via the Internet at http://pubs.acs.org.

References

(1) Chan, W.; Nie, S. *Science* **1998**, *281*, 2016–2018.
(2) Bruchez, J.; Moronne, M.; Gin, P.; Weiss, S.; Alivisatos, A. *Science* **1998**, *281*, 2013–2016.
(3) Bharali, D. J.; Lucey, D. W.; Jayakumar, H.; Pudavar, H. E.; Prasad, P. N. *J. Am. Chem. Soc.* **2005**, *127*, 11364–113671.
(4) Jaiswal, J.; Mattoussi, H.; Mauro, J.; Simon, S. *Nat. Biotechnol.* **2003**, *1*, 47–57.
(5) Huynh, W.; Dittmer, J.; Alivisatos, A. *Science* **2002**, *295*, 2425–2427.
(6) Sun, B.; Marx, E.; Greenham, N. *Nano Lett.* **2003**, *3*, 961–963.
(7) Gur, I.; Fromer, N.; Chen, C.; Kanaras, A.; Alivisatos, A. *Nano Lett.* **2007**, *7*, 409–414.
(8) Park, J.; Joo, J.; Kwon, S.; Jang, Y.; Hyeon, T. *Angew. Chem., Int. Ed* **2007**, *46*, 4630–4660.
(9) Embden, J.; Jasieniak, J.; Gómez, D.; Mulvaney, P.; Giersig, M. *Aust. J. Chem.* **2007**, *60*, 457–471.
(10) Xie, R.; Battaglia, D.; Peng, X. *J. Am. Chem. Soc.* **2007**, *129*, 15432–15433.
(11) Gerbec, J.; Magana, D.; Washington, A.; Strouse, G. *J. Am. Chem. Soc.* **2005**, *127*, 15791.
(12) Adam, S.; Talapin, D.; Borchert, H.; Lobo, A.; McGinley, C.; de Castro, A.; Hasse, M.; Weller, H.; Möller, T. *J. Chem. Phys.* **2005**, *123*, 084706.
(13) Borchert, H.; Haubold, S.; Haase, M.; Weller, H.; McGinley, C.; Riedler, M.; Moller, T. *Nano Lett.* **2002**, *2*, 151–154.
(14) Oda, K. *Industrial Health* **1997**, *35*, 61–68.
(15) Zheng, W.; Winter, S. M.; Kattnig, M. J.; Carter, D. E.; Sipes, I. G. *J. Toxicol. Environ. Health* **1994**, *43*, 483–494.
(16) Kabe, I.; Kazuyuki, O.; Hiroshi, N.; Nomiyama, T.; Uemura, T.; Hosoda, K.; Ishizuka, C.; Yamazaki, K.; Sakurai, H. *J. Occup. Health* **1996**, *38*, 6–12.
(17) Yamazk, I.; Tanaka, A.; Hirata, M.; Omura, M.; Makita, Y.; Inoue, N.; Sugio, K.; Sugimachi, K. *J. Occup. Health* **2000**, *42*, 169–178.
(18) Haubold, S.; Haase, M.; Kornowski, A.; Weller, H. *ChemPhysChem.* **2001**, *2*, 331–334.
(19) Micic, O.; Sprague, J.; Lu, Z.; Nozik, A. *Appl. Phys. Lett.* **1996**, *68*, 3150–3152.
(20) Talapin, D.; Gaponik, N.; Borchert, H.; Rogach, A.; Haase, M.; Weller, H. *J. Phys. Chem. B* **2002**, *106*, 12659–12663.
(21) Antonietti, M.; Kuang, D.; Smarsly, B.; Zhou, Y. *Angew. Chem., Int. Ed.* **2004**, *43*, 4988–4992.
(22) Kappe, O. *Angew. Chem., Int. Ed.* **2004**, *43*, 6250–6284.
(23) Redel, E.; Thomann, R.; Janiak, C. *Chem. Commun.* **2008**, 1789–1791.
(24) Laali, K.; Gettwert, V. *J. Fluorine Chem.* **2001**, *107*, 31–34.
(25) Koval'chuk, E.; Reshetnyak, O.; Kozlovs'ka, Z.; Bła˙ejowski, J.; Gladyshevs'kyj, R.; Obushak, M. *Thermochim. Acta* **2006**, *444*, 1–5.
(26) Heredia-Moya, J.; Kirk, K. *J. Fluorine Chem.* **2007**, *128*, 674–678.
(27) Fox, D.; Gilman, J.; De Long, H.; Trulove, P. *J. Chem. Thermodynamics* **2005**, *37*, 900–905.
(28) An important set of controls were also run on the IL's (hmim, bmpy, and TBA) with a chloride counterion. In all reactions, the chloride salt resulted in precipitation of the In precursor, presumably due to facile formation of $InCl_3$.
(29) Aki, S.; Brennecke, J.; Samanta, A. *Chem. Commun.* **2001**, 413–414.
(30) Lide, D.; *CRC Handbook of Chemistry and Physics, 88th ed.,* 2007−2008.
(31) Pi, X.; Mangolini, L.; Campbell, S.; Kortshagen, U. *Phys. Rev. B* **2007**, 085423.
(32) Washington, A.; Strouse, G. *J. Am. Chem. Soc.* **2008**, ASAP.

NL802075J